

Synthesis of Some New 4-methylpiperazin-1-yl-methyl-4H-1,2,4-triazole-3- thiol Derivatives of Expected Anticancer and Antimicrobial Activity

YILDIZ UYGUN CEBECİ (✉ yildizuygun41@hotmail.com)

Kırklareli University

Sengül Alpay Karaoğlu

Recep Tayyip Erdoğan University

Muhammed Altun

Cankiri Karatekin University

Research Article

Keywords:

Posted Date: December 15th, 2022

DOI: <https://doi.org/10.21203/rs.3.rs-2373014/v1>

License:  This work is licensed under a Creative Commons Attribution 4.0 International License.

[Read Full License](#)

Additional Declarations: No competing interests reported.

Synthesis of Some New 4-methylpiperazin-1-yl-methyl-4H-1,2,4-triazole-3-thiol Derivatives of Expected Anticancer and Antimicrobial Activity

Yildiz Uygun Cebeci¹ Sengül Alpay Karaoglu² Muhammed Altun³

¹*Department of Chemistry, Kırklareli University, Kırklareli, Turkey*

²*Department of Biology, Recep Tayyip Erdoğan University, Rize, Turkey*

³*Faculty of Science, Department of Chemistry, Cankiri Karatekin University, Cankiri, Turkey*

Abstract

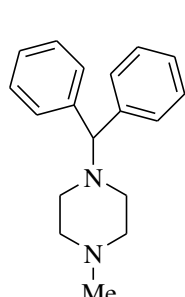
Different series of annulated methylpiperazine derivatives were designed, synthesized traditional methods, and structurally characterized. 1,2,4-Triazole-fluoroquinolone and 1,2,4-triazole-conazole hybrids are designed, synthesized, and investigated in vitro against a variety of common diseases. The structure of the newly synthesized compounds are characterized from spectral data (IR, ¹H NMR, ¹³C NMR, and LC-MS). The antibacterial activity against both Gram-positive and Gram-negative bacteria is shown to be enhanced by many of the produced compounds. Also, some of the products are found to have strong antiproliferative effects against HeLa cervical cancer cells, whilst demonstrating cytotoxic effects toward normal cells. Compounds **6d** and **6e** showed intermediate anticancer activity

Introduction

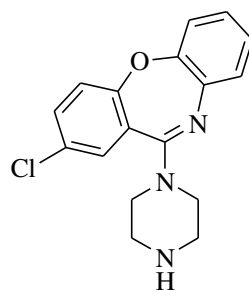
The World Health Organization ranks cervical cancer as the fourth most frequent malignancy in women, and it has the third highest fatality rate [1]. According to a report issued by the WHO, cervical cancer accounts for around 12% of all kinds of cancers that can occur in women and is more prevalent in countries that are still developing [2]. Low success has been achieved in the treatment of cervical cancer with drugs and it has been observed that it has quite a lot of side effects [3]. In order for advancements to be made in early detection and improved efficacy of available chemotherapeutic approaches in the field of cervical cancer research [4, 5], there needs to be a constant search for safer new chemical moieties with significant anticancer activity, and identification of efficient cellular targets is required for the effective treatment of cancer [6].

Piperazines are compounds that have a wide range of uses in pharmaceutical chemistry and are of great biological importance [7-17]. Piperazine compounds are in the structure of many

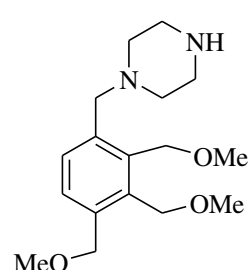
antifungal and antibacterial drugs [18-21]. After a piperazine compound was used in the structure of the anthelmintic compound, it took place in the structure of many compounds [22, 23]. The piperazine scaffold has been recognized as an important component of a wide variety of naturally active chemicals found in pharmaceutical drugs [24-27]. Antibacterial, antituberculosis, anticancer, antiviral, antiinflammatory, antipsychotic, anti- Alzheimer's, antifungal, and antidiabetic properties have been attributed to piperazine and its derivatives [28–31]. Anticonvulsant, antimalarial, and antianalgesic activities have also been attributed to piperazine and its derivatives. In Figure 1 are depicted numerous drugs with this pattern as a fundamental structural property.



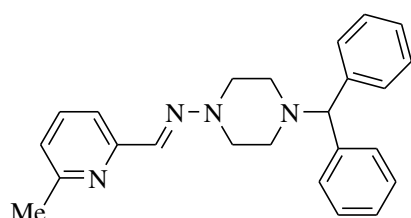
Cyclizine (Antihistaminic)



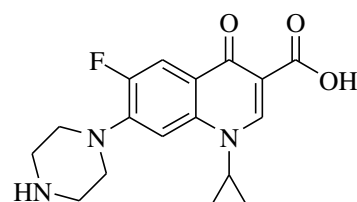
Amoxapine (Antidepressant)



Trimetazidine (Antischemic)

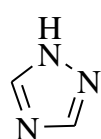


Ropizine (Anticonvulsant)

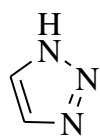


Ciprofloxacin (Antibiotic)

The remarkable heterocyclic structure known as the five-membered triazole is distinguished from other such structures by its one-of-a-kind structural characteristics. Triazoles are a type of diunsaturated ring structure that include three nitrogen atoms. They are also known by the name pyrrodiazoles. There are two possible isomeric configurations for triazoles, which are referred to as 1,2,3-triazole and 1,2,4-triazole respectively [32]. These configurations differ in the position of the nitrogen atoms (figure 2).



1,2,4-Triazole



1,2,3-Triazole

Because of their remarkable pharmacophoric qualities, compounds of 1,2,4-triazole have been a subject of research for drug design over the past decade [33]. Because of the electron-rich essence of 1,2,4-triazoles, they are able to interact with a wide range of biochemical aims and enzymes, which enables them to display a diverse array of biological activities. Some of these activities include antibacterial, antifungal, antitumor, anti-inflammatory, antitubercular, hypoglycemic, antidepressant, anticonvulsant, analgesic, antiviral, anticancer, antimalarial, antioxidant etc. [34-37]. The application of 1,2,4-triazoles in the development of new molecules has seen a remarkable development over the period of recent history. The several medicines containing triazole are available on the market, and they can be utilized for a diverse range of purposes (figure 3)

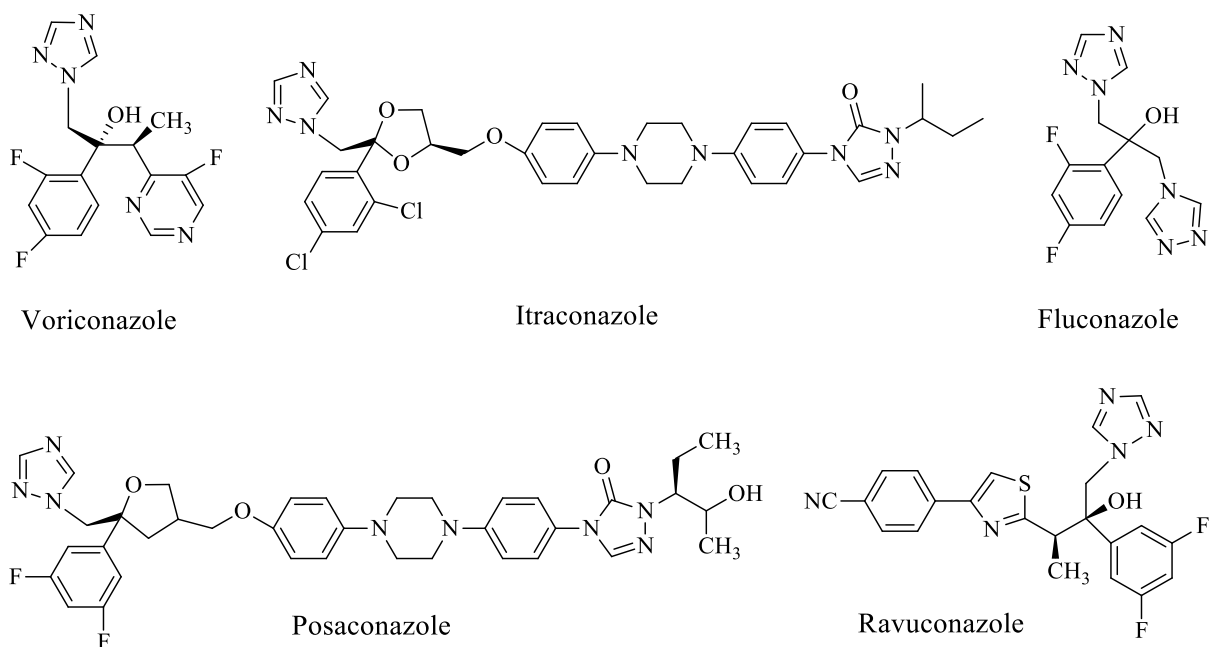


Figure 3. Some known azole class antifungals.

The field of molecular hybridization, which is based on the incorporation of two or more pharmacophore moieties into a single framework by means of a linker, has recently attracted a significant amount of research. This modification has the ability to create compounds of the homodimer or heterodimer type. The primary purpose is to enhance the effectiveness of the drug while simultaneously minimizing its adverse effects and preventing drug resistance [38-41].

By hybridizing 1,2,4-triazole ring systems with piperazine, the purpose of this research was to create novel heterocycles that have the properties of hybrid molecules and can be synthesized.

In this study, we reported the synthesis of basic Mannich base and conazole derivatives, antimicrobial and anticancer properties were investigated.

Antimicrobial Activity Assessment

The Hifzissihha Institute of Refik Saydam in Ankara, Turkey, was the source of the test microorganisms, which were as follows: *E. coli* ATCC35218, *Y. pseudotuberculosis* ATCC911, *P. Aeruginosa* ATCC43288, *E. Faecalis* ATCC29212, *S. aureus* ATCC25923, *B. Cereus* 709 Roma, *M. smegmatis* ATCC607, *C. Albicans* ATCC60193 and *S. cerevisiae* RSKK 251. In order to make a 20.0 g mL⁻¹ solution, each substance was weighed and dissolved in dimethylsulfoxide. The antibacterial activity of the compounds was quantified in the appropriate broth media using double microdilution, and the MIC values (g mL⁻¹) were calculated. The antibacterial and antifungal experiments were conducted in Mueller-Hinton broth (MH) (Difco, Detroit, MI, USA) at a pH of 7,3 and buffered Yeast Nitrogen Base (YNB) at a pH of 7.0, respectively. Microdilution test plates were incubated at 35 °C for 18–24 h. *M. smegmatis* was cultured in Brain Heart Infusion broth (BHI) (Difco, Detroit, MI, USA) for 48–72 h at 35 °C [42]. Fluconazole (5 µg) and ampicillin (10 µg) were the typical antibacterial and antifungal medications. The solvent control was DMSO diluted to 1:10 in order to ensure the correct concentration.

Cell Culture and Cell Proliferation Tests

Cell Culture

The sterile cabinet was used for all of the experiments testing for antiproliferative activity. Sterilized culture flasks with spent DMEM were discarded. The cells were cultured in a flask and 10 mL of trypsin-EDTA was added. Closing the flask and placing it in a CO₂ incubator (5% CO₂) at 37 °C for 1-2 minutes. Therefore, the surface was cleansed of any cells that had been sticking to it. After incubation, 10 mL of fresh medium (DMEM) was added to the container to restore the original pH level. Two 15-mL falcon tubes were each filled with an equal amount of the cell suspension. To get the cells to the bottom of the tube, we centrifuged it at 600 rpm for 5 minutes. After centrifugation, 3 mM of medium was added to the cell debris and the remaining liquid was discarded from the falcon tube. A sterile pipette was used to disperse cells that had settled to the bottom of the tube. Cells were counted using a Cedex Hires Analyzer (made by Roche). The cells that had already died were stained with trypan blue. The collected information was utilized to establish the cell density in each well of the E-Plate 96 plate.

Antiproliferative Activity Tests

Measurements of antiproliferative activity were taken with a real-time cell analyzer (xCelligence RTCA SP, ACEABIO, Inc.). The foundation of RTCA SP is the use of microelectronic technology to track cellular processes. E-Plate 96 and the RTCA SP (Single Plate) unit's other parts include a control unit and an analyzer. The plate with 96 wells is a crucial component of the RTCA SP (E-Plate 96). A microelectronic cell sensor array designed for cell adhesion is located at the base of the plate. Changes in the cellular resistance are detected by the RTCA SP sensors as a result of cellular biology.

To enable analysis, this recorded change in resistance is transformed from analog to digital signals. Electrode resistance is affected by a variety of factors, including cell viability, cell number, cell shape, and the attraction of molecules to each other (adhesion). When cells are present at an electrode, they act as insulators and raise the medium's resistance. Consequently, the bigger the number of cells on the electrode, the larger the resulting shift in resistance. It is the relative position of the cell state that provides the basis for the cell index (CI, Cell Index) parameter. When cells are absent or not strongly connected to the electrodes, the CI value is close to zero. The CI value increases [43] if more cells are coupled to the electrode under the same physiological conditions. The Cell Index (CI) has no inherent units. Increasing CI indicates that cells are adhering to the surface, maturing, exhibiting little morphological change, and proliferating. So, if the CI value rises, it means there are no issues with cell shape, stress, environment, or proliferation.

Every well of an E-Plate 96 has been pre-filled with a certain volume of medium, and the cells are plated in these wells. The cells quickly reach the bottom of the wells, where a sensor-electrode is placed, and cling to its surface. The station, housed inside a CO₂ incubator, is used to track changes in the electrical properties of the sensor surfaces. The RTCA software in the RTCA analyzer and the control unit simultaneously determines quantitative information on the biological state of the cell, including cell viability, morphology, and cytotoxicity. Studies of antiproliferative activity were performed using Abay's [44] methodology. The samples were diluted in sterile DMEM and then dissolved in sterile DMSO (at a concentration of 20 mg/mL) (1:20). Each well of an E-plate 96 had 50 l of culture medium (DMEM) poured into it. After 15 minutes in the CO₂ incubator, the plate was incubated in the sterile cabinet (for the thermal balance). After that, we ran a background check on the plate using the RTCA station.

E-plate 96's status was determined after this one-minute reading. Using the cell counting apparatus, we determined how many cells to put to the wells, and we prepared the solution.

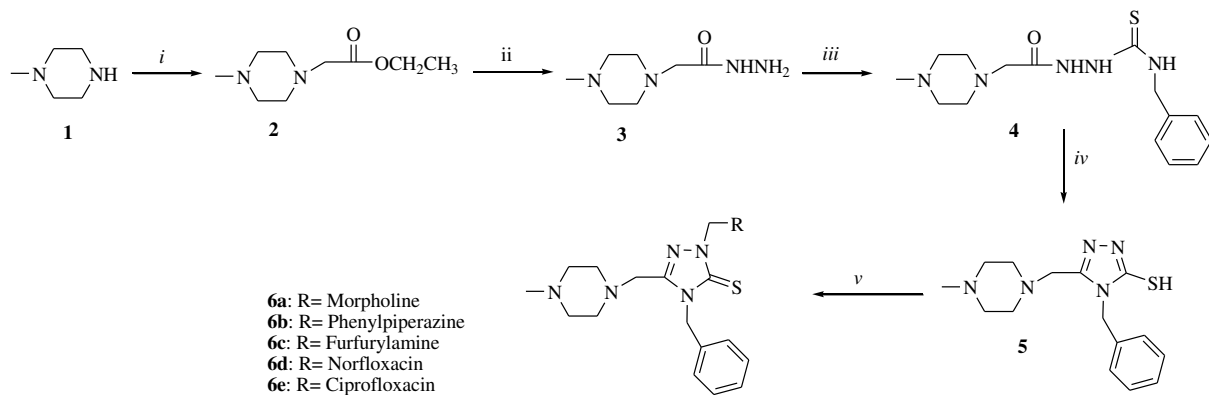
Each well in the plate received 100 μ l of this cell solution (25,000 cells/well) except for the last three wells. These wells were left empty in order to determine whether or not DMEM may affect CI. The second phase (80 minutes) began once the plate was reinserted into the RTCA station. This gave the cells time to settle to the bottom of the well and begin the process of proliferation. After this time had elapsed, the e-plate was returned to the sterile cabinet, where the growth medium solution containing the molecular samples was added to the wells at varying concentrations. Three separate sample solutions (100, 50, and 10 g/mL) were introduced to the wells. Each well had its volume brought up to 200 μ l with DMEM. Three independent tests were performed on each dose. Next, the RTCA's plate was secured for the final time. For 48 hours, the cells' states of life and death were tracked. RTCA Software examined the variation in well triplicates by calculating the standard deviation.

Results And Discussion

Chemistry

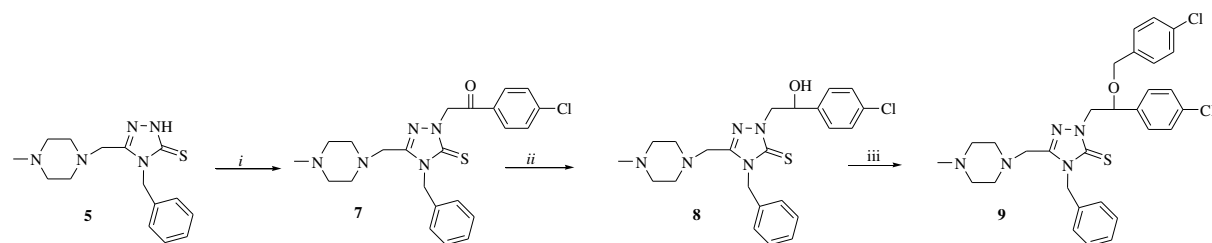
In this study, there is starting material Methylpiperazine. Methylpiperazine was reacted with ethyl bromoacetate and hydrazinhydrate to afford the corresponding asetohydrazide compounds (**3**) then hydrazide molecule (**3**) was converted to carbox(thio)amide derivative (**4**), followed by an intramolecular cyclization reaction to obtain 1,2,4-triazoles (**5**) (Scheme 1). This compound was characterized by the presence of a signal at 13.90 ppm in the ^1H NMR data as a D_2O exchangeable singlet confirming the existence of a -SH function. The stretching band derived from these groups appeared at 2935 cm^{-1} , at the FT-IR data of this molecule.

Mannich bases are physiologically reactive agents [45-47]. Mannich bases (**6a-e**) were obtained by treatment of compound (**5**) with formaldehyde and several biologically active amines (Scheme 1) [48, 49].



Scheme 1: *i.* $\text{BrCH}_2\text{COOEt}$, EtOH ; *ii.* NH_2NH_2 , EtOH ; *iii.* RNCS , EtOH , *iv.* NaOH , EtOH , H_2O ; *v.* dimethyl formamide, seconder amine, room temperature, 24 h.

Alkylation of compound (**5**) with 2-bromo-1-(4-chlorophenyl) ethanone in ethanol afforded the corresponding compound (**7**). NH proton attached to the triazole group disappeared for compound (**5**) at the ^1H NMR spectra. New aromatic peaks were resonated in the region 7.20-7.35 ppm. In ^{13}C NMR data of molecules, the carbon atom ($\text{C}=\text{O}$) was observed between 171.10 ppm for the newly added carbonyl group. The reduction of carbonyl group with NaBH_4 in (**7**) to alcohol gave compound (**8**) which, again, was achieved using classical heating. Looking at compound number (**8**) the carbonyl group peak has evanesced at the ^{13}C NMR data and OH peak added between 5.26 ppm in the ^1H NMR. The spreading band obtained in this group (OH) appeared at 3319 cm^{-1} , in the FT-IR data of molecule. The synthesis of compound (**9**) was achieved by treatment of compound (**8**) with substituted benzyl chlorides, namely 4-chloro-benzyl chlorides in the presence of NaH . (Scheme 2). In both FT-IR and ^1H NMR data of the molecule, the peaks due to the -OH group have disappeared. Other peaks approving molecule structures were displayed at the concerned chemical ranges in the ^1H NMR and ^{13}C NMR spectra. Moreover, $[\text{M}+1]$ ion signals were appeared at the concerned m/z ranges auxiliary the offered structure of molecule (**9**) (Scheme 2).



Scheme 2: *i.* 2-Bromo-1-(4-chlorophenyl)ethanone, NaOEt , reflux,; *ii.* NaBH_4 , EtOH , reflux; *iii.* 4-chlorobenzylchloride, THF , NaH , reflux,

Antimicrobial Activity

Table 1 displays the results of antimicrobial activity testing performed on all novel products using the minimal inhibition concentration (MIC) approach. Compounds (2-9) were examined for their ability to inhibit the growth of four different bacteria and three different yeasts. Compounds (2, 5, 6a-e, and 7-9) had moderate activity against the tested microorganisms, while compounds (3, 4, and 5) showed stronger activities against *M. smegmatis*, *Y. pseudotuberculosis*, and *E. coli*. That means that compounds (2) and (9) are more effective against *M. smegmatis* than the other molecules, with MIC values of 7.81 g/mL and respectively. The Mannich bases (6a, 6d, and 6e) showed the best and most effective activity against both gram-positive and gram-negative bacteria, with MIC values of 0.24 g/mL, but they had no effect on yeast strains. At the same time, when compared to the standard drug *Streptomycin*, these compounds were much better at killing *M. smegmatis* than *Streptomycin*. The conazole derivative compound (9) showed only moderate efficacy against both gram-positive and gram-negative bacteria and yeasts.

Table 1. Screening for antimicrobial activity of the compounds (μg/μl).

No	Stoc. μg/ml	Microorganisms and Minimal Inhibition Concentration								
		Ec	Yp	Pa	Sa	Ef	Bc	Ms	Ca	Sc
2		7.81	7.81	31.2 5	31.25	62.5	31.25	7.81	-	-
3		-	-	-	-	-	-	-	-	-
4		-	-	-	-	-	-	-	-	-
5		-	-	-	125	-	-	-	250	125
6a		<0.24	<0.24	<0.2 4	<0.24	<0.24	<0.24	<0.2 4	-	125
6b		125	125	-	-	-	-	-	-	-
6c		125	125	-	-	-	-	-	-	-
6d		<0.24	<0.24	<0.2 4	<0.24	<0.24	<0.24	<0.2 4	62.5	15.65
6e		<0.24	<0.24	<0.2 4	<0.24	<0.24	<0.24	<0.2 4	62.5	15.65
7		62.5	125	-	62.5	-	125	15.65	125	62.5
8		31.25	125	-	500	-	125	62.5	125	62.5
9		125	125	125	125	-	125	7.81	125	125
DMS O		125	125	125	-	-	500	125	500	-
Amp.		10	18	>128	35	10	15			

Strep.								4		
Flu								<8	<8	

Ec: *Escherichia coli* ATCC 25922, Yp: *Yersinia pseudotuberculosis* ATCC 911, Pa: *Pseudomonas aeruginosa* ATCC 27853, Sa: *Staphylococcus aureus* ATCC 25923, Ef: *Enterococcus faecalis* ATCC 29212, Bc: *Bacillus cereus* 702 Roma, Ms: *Mycobacterium smegmatis* ATCC607, Ca: *Candida albicans* ATCC 60193, *Saccharomyces cerevisiae* RSKK 251, Amp.: Ampicillin, Str.: Streptomycin, Flu.: Fluconazole, (—): no activity

Anticancer Activity

Abay's [44] method was used to test the molecules' potential antiproliferative activity against HeLa cells. The samples' antiproliferative activity ranged throughout 3 doses (Figure 1 and Figure 2). The wells that did not contain the molecules samples resulted in a high Cell Index (red line). In the wells where the molecules were introduced, CI values dropped. Only DMEM medium was added to the last three wells. A assessment was established using these three wells. No change in impedance was detected in the DMEM-only wells. For these three wells, the Cell Index (CI) values remained constant throughout the experiment (green line). The red line represents the CI values obtained from wells containing only DMEM and cells. The rapidly increasing CI can be directly attributed to the unimpeded proliferation of HeLa cells. This demonstrates that there is no negative proliferation effect when cells are attached to gold-plated microelectrodes in a well-ground experiment. The impedance shift is proportional to the number of cells that have adhered to the bottom electrodes of the plate. In turn, the CI value rises as a consequence of this. However, a drop in CI value indicates that cell growth is being restrained. The transfer of the e-Plate 96 from the RTCA station in the incubator (95% CO₂, 37 °C) to the sterile cabinet and the subsequent addition of the sample account for the sharp drop in CI observed at the 2-hour mark. Once the molecular samples had been added, the E-Plate 96 was placed back into the CO₂ incubator's station. The CI values for cells in wells where no samples were added rose sharply (red line). However, the molecules from the samples significantly inhibited cell growth in the wells where they were introduced. Because of this, the CI values were quite low.

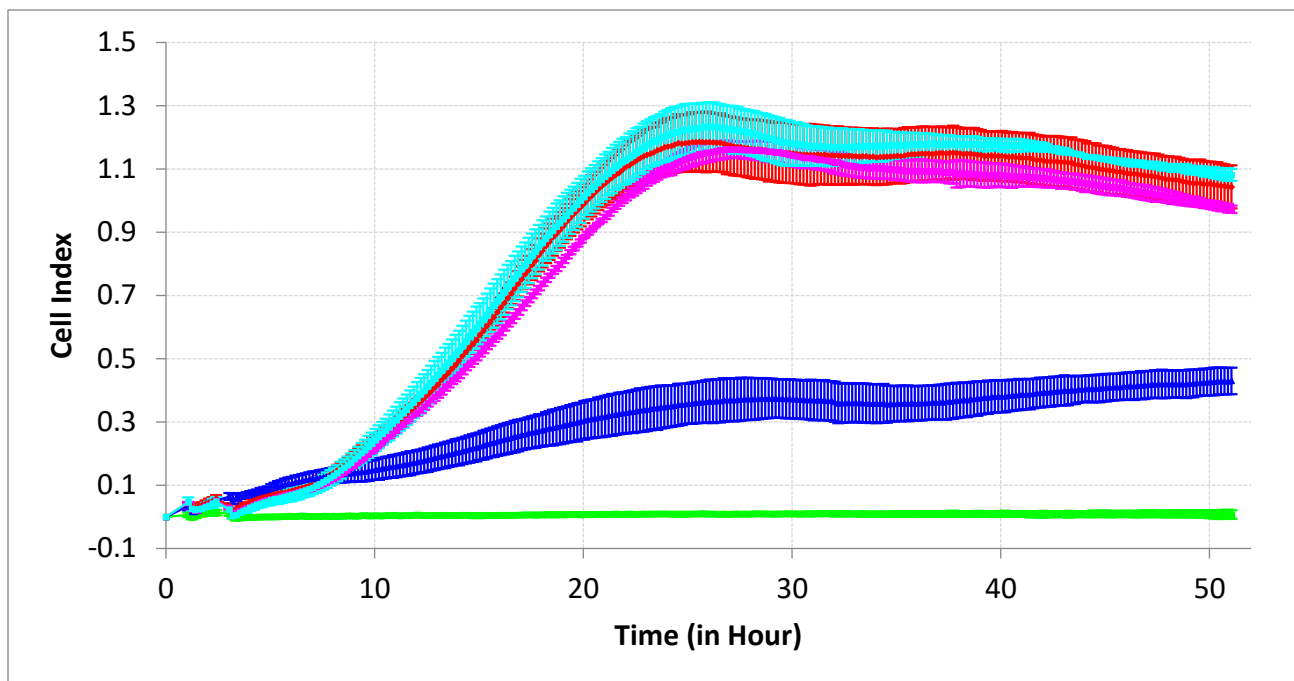


Figure 1. Time-CI (Cell Index) plot showing the antiproliferative activity test results of compound 6d against HeLa cell line (the concentration unit is $\mu\text{g/mL}$).

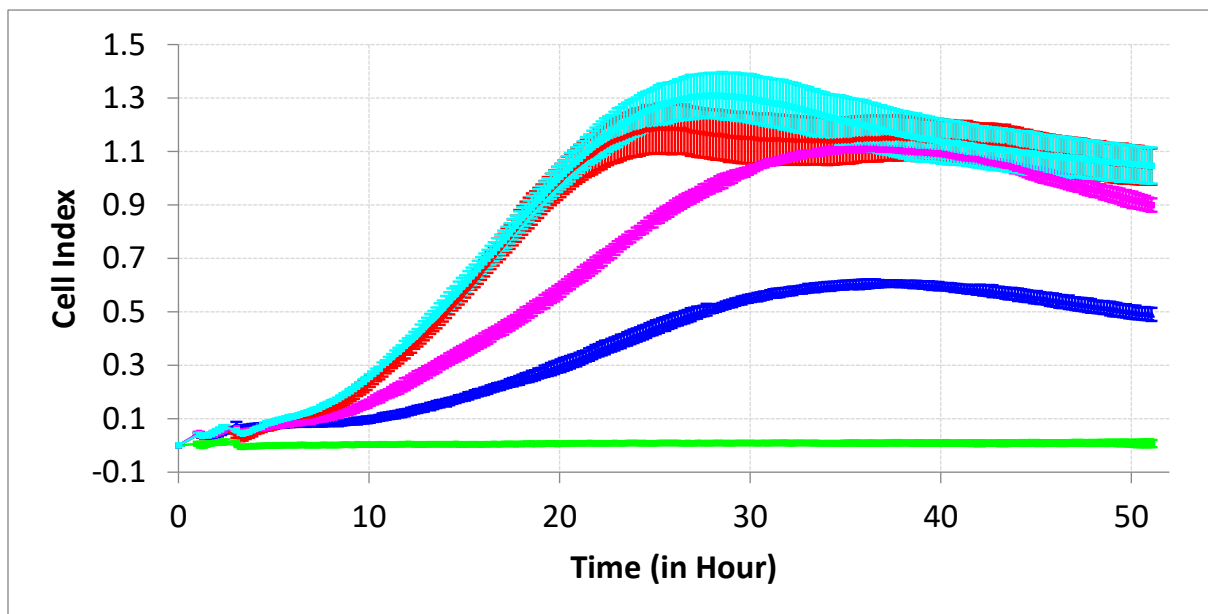


Figure 2. Time-CI (Cell Index) plot showing the antiproliferative activity test results of compound 6e against HeLa cell line (the concentration unit is $\mu\text{g/mL}$).

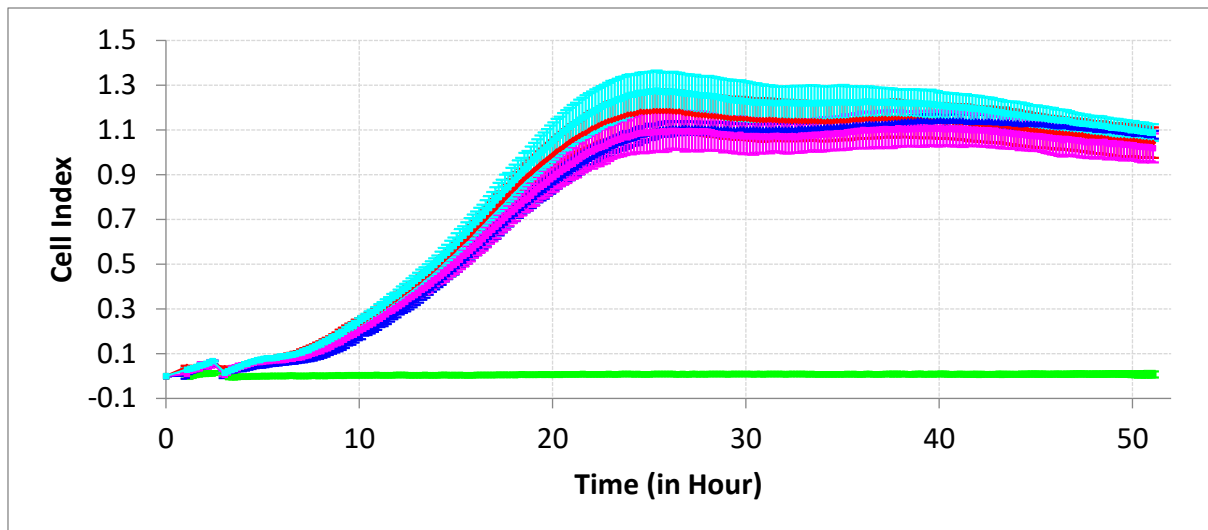


Figure 3. Adding different doses of DMSO to HeLa cell wells (the concentration unit is $\mu\text{g/mL}$).

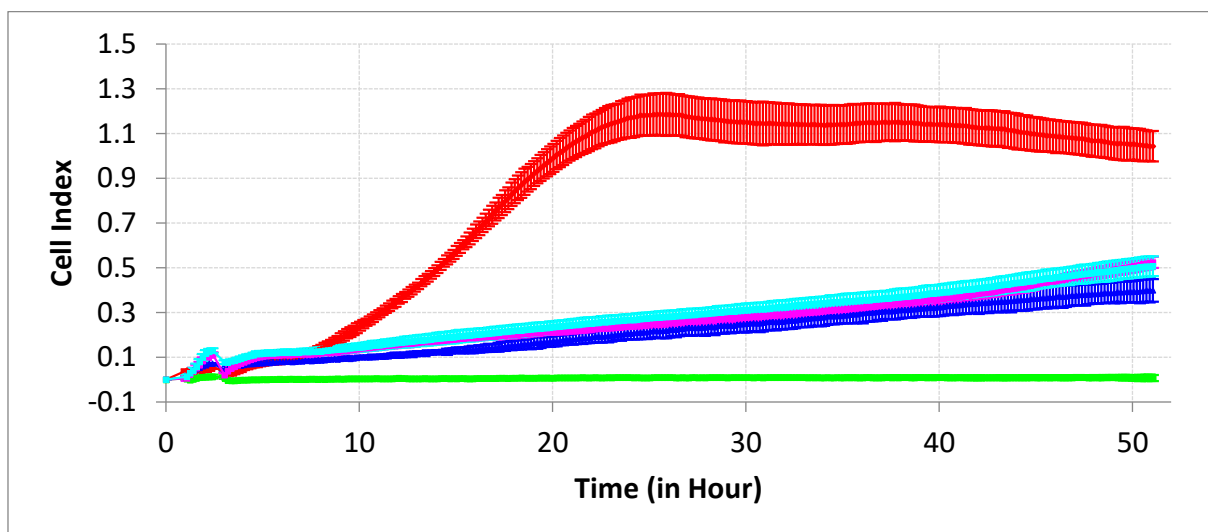


Figure 4. Effect of all 5FU doses used as positive control (the concentration unit is $\mu\text{g/mL}$).

The eplate was transferred to the sterile cabinet 80 minutes after the cells were added to the wells. Wells were prepared with 100, 50, and 10 g mL^{-1} sample concentrations. There were three separate assessments of each sample dose. We tracked the molecules' antiproliferative effect on HeLa cells in real time for 48 hours, measuring their performance every 10 minutes. Standard deviations for the well mean CI values are displayed as vertical bars in the xCelligence RTCA SP software.

Investigating the dose effect requires thinking about concepts like hormesis and inverse hormesis as well as dose-dependent effects and dose-dependent reverse effects. [42–44] Figures 1 and 2 display the inhibitory effects of these molecules on HeLa cell proliferation. The CI

values measured in cell-free wells rose sharply (red line). No DMSO-induced antiproliferative activity was detected when HeLa cells were cultured in the presence of varying concentrations of DMSO (Figure 3). All doses of 5FU used as a positive control had a sizable effect, and the values for the CI were all very close. No antiproliferative effect was seen at concentrations of the molecules below 10 g mL^{-1} (turquoise line). The CI from the low doses of the molecules was equivalent to that from the placebo group. At the end of the experiment, only the low dose of compound **6d** was significantly different from the control group (after 35 hours). A net antiproliferative effect cannot be inferred from the current circumstances. Figure 4 shows a graph of 5FU, which is used as a positive control, and it is clear that the CI for the low dose (turquoise line) is significantly different from the CI values shown in red (negative control). Strong antiproliferative activity was observed at middle doses of **6d** and **6e** molecules (50 g mL^{-1} , pink line). Their antiproliferative activity was consistent throughout the study. Additionally, it has been discovered that high concentrations of molecules have potent antiproliferative effects. The **6e** molecule exhibited potent antiproliferative activity at high concentrations (100 g mL^{-1} , dark blue line). The **6d** molecule had a potent antiproliferative effect on HeLa cells even at high concentrations (100 g mL^{-1} ; dark blue line). Extremely high concentrations of **6e** molecules produced CI values that were identical to the CI values of wells in which no cells had been added (green line). The experiment's strong effect persisted throughout. To a greater extent than with any other molecules, the dose-effect differences of **6d** and **6e** were observed. The structural forms of these molecules are responsible for their antiproliferative effects. Antiproliferative activity potentials of molecules showing no or weak effect against HeLa cells should be examined and their effects should be investigated against other cancer cell lines.

Experimental

Chemistry

Fluka Chemie AG (Buchs, Switzerland) supplied the chemicals, which were purchased and used as-is. All melting points were measured in open capillaries using a Büchi B-540 melting point apparatus and have not been adjusted for temperature. TLC was used to track reactions on aluminum sheets coated with silica gel 60 F254. Detection was done with UV light, and the mobile phase was composed of ethyl acetate and diethyl ether (1:1). The FT-IR spectra were obtained with a Perkin Elmer 1600 series spectrometer. Spectra were recorded in DMSO-d6 using a Bruker Avane II 400 NMR spectrometer for ^1H NMR and

¹³C NMR (400 MHz for ¹H and 100 MHz for ¹³C). Quattro GC-MS (70 eV) instrument was used to collect the electron ionization (EI) mass spectra.

Methyl (4-methylpiperazin-1-yl)acetate (2)

To a solution of the methylpiperazin (10 mmol) in tetrahydrofuran, triethylamine (20 mmol) and ethyl bromoacetate (10 mmol) were added and the mixture was stirred at room temperature for 24 hours. The precipitate was removed by filtration and the resulting solution was evaporated under reduced pressure to dryness. The crude product obtained was purified by column chromatography (silica gel, hexane/ethyl acetate 7:3).

Yield: % 89, m.p: 85-87°C. FT IR (ν_{max} , cm⁻¹): 1734 (C=O). ¹H NMR (DMSO-*d*₆, δ ppm): 1.17-1.20 (3H, m, CH₃), 1.99 (2H, s, CH₂), 2.14 (2H, s, CH₂), 2.30 (2H, s, CH₂), 3.17 (2H, s, CH₂), 3.39 (2H, s, CH₂), 4.06-4.10 (3H, m, CH₃). ¹³C NMR (DMSO-*d*₆, δ ppm): 14.57 (CH₃), 46.17 (CH₃), 53.24 (CH₂), 55.06 (CH₂), 58.98 (CH₂), 60.20 (CH₂), 63.93 (CH₂), 170.36 (C=O). EI MS *m/z* (%): 173.25 ([M+1]⁺, 100), 195.40 ([M+Na]⁺, 70).

2-(4-methylpiperazin-1-yl)acetohydrazide (3)

A solution of compound 2 (10 mmol) in ethanol was refluxed with hydrazine hydrate (25 mmol) for 15 h. The crude product obtained was purified by column chromatography (silica gel, hexane/ethyl acetate 7:3).

Yield: % 85, m.p: 134-136°C. FT IR (ν_{max} , cm⁻¹): 1734 (C=O). ¹H NMR (DMSO-*d*₆, δ ppm): 2.14 (3H, s, CH₃), 2.30 (2H, s, CH₂), 2.40 (4H, s, 2CH₂), 2.88 (4H, s, 2CH₂), 3.75 (2H, brs, NH₂), 8.84 (1H, s, CH₂). ¹³C NMR (DMSO-*d*₆, δ ppm): 46.20 (CH₃), 53.21 (2CH₂), 55.01 (2CH₂), 60.37 (CH₂), 168.69 (C=O). EI MS *m/z* (%): 173.89 ([M+1]⁺, 100), 195.75 ([M+Na]⁺, 75).

***N*-benzyl-2-[(4-methylpiperazin-1-yl)acetyl]hydrazinecarbothioamide (4)**

A mixture of compound 3 (10 mmol) and the corresponding benzyliso(thio)cyanate (10 mmol) in dichloromethane was stirred at room temperature for 24 h. The solid precipitate was collected by filtration and recrystallized from ethanol to afford the desired compound.

Yield: % 81, m.p: 139-141°C. FT IR (ν_{max} , cm^{-1}): 3057 (aromatic CH), 3117 (NH), 3218 (NH), 1703 (C=O). ^1H NMR (DMSO- d_6 , δ ppm): 1.86 (3H, s, CH_3), 2.00 (2H, s, CH_2), 2.17 (2H, s, CH_2), 2.36 (2H, s, CH_2), 2.47 (2H, s, CH_2), 3.02 (2H, s, CH_2), 4.72 (2H, s, CH_2), 7.22-7.32 (5H, m, arH), 8.38 (1H, s, NH), 8.50 (1H, s, NH), 9.30 (1H, s, NH). ^{13}C NMR (DMSO- d_6 , δ ppm): 45.97 (CH_3), 47.19 (CH_2), 47.40 (CH_2), 52.97 (CH_2), 54.81 (CH_2), 60.19 (CH_2), 63.96 (CH_2), arC: [127.08 (CH), 127.48 (CH), 127.74 (CH), 128.44 (CH), 128.51 (CH), 139.70 (C)], 169.58 (C=O), 182.63 (C=S). EI MS m/z (%): 322.45 ([M+1] $^+$, 100), 201.26 (89), 178.10 (67), 166.10 (43).

4-benzyl-5-[(4-methylpiperazin-1-yl)methyl]-4*H*-1,2,4-triazole-3-thiol (5)

The solution of the corresponding compound 4 (10 mmol) in ethanol:water (1:1) was refluxed in the presence 100 mL of 2% NaOH for 6h.

Then the resulting solution was cooled to room temperature and acidified to pH 4 with 37% HCl.

The precipitate formed was filtered off, washed with water and recrystallized from ethyl acetate to afford the desired compound.

Yield: % 71, m.p: 155-157°C. FT IR (ν_{max} , cm^{-1}): 3071 (aromatic CH), 2935 (SH). ^1H NMR (DMSO- d_6 , δ ppm): 2.17 (3H, s, CH_3), 2.61 (2H, s, CH_2), 4.29 (2H, d, J = 8.0 Hz, CH_2), 5.11 (2H, s, CH_2), 5.19 (2H, s, CH_2), 5.24 (2H, s, CH_2), 5.32 (2H, s, CH_2), 7.20-7.35 (5H, m, arH), 13.90 (1H, s, SH). ^{13}C NMR (DMSO- d_6 , δ ppm): 11.72 (CH_3), 44.68 (CH_2), 45.83 (CH_2), 46.16 (CH_2), 46.65 (CH_2), 51.52 (CH_2), 52.69 (CH_2), arC: [127.68 (CH), 127.92 (CH), 128.23 (CH), 128.58 (CH), 128.79 (CH), 152.53 (C)], 164.84 (triazole C-3), 167.56 (triazole C-5).

General Method for The Synthesis of Compounds 6a-e

To a solution of corresponding compound 5 (10 mmol) in dimethyl different amines was added and the mixture was stirred at room temperature in the presence of formaldehyde (30 mmol) for 24 h. The solid precipitate was collected by filtration, washed with water and recrystallized from dimethylsulfoxide:water (1:1) to give the desired compound.

4-benzyl-5-((4-methylpiperazin-1-yl)methyl)-2-(morpholinomethyl)-2H-1,2,4-triazole-3(4H)-thione (6a)

Yield: % 83, m.p: 178-180 °C. FT IR (ν_{max} , cm^{-1}): 3088 (aromatic CH), 1593 (C=N). ^1H NMR (DMSO- d_6 , δ ppm): 2.78 (3H, s, CH_3), 3.37 (10H, s, 5 CH_2), 3.59 (10, s, 5 CH_2), 5.04 (2H, s, CH_2), 6.94 (1H, s, arH), 7.24-7.28 (1H, m, arH), 7.47 (1H, s, arH), 7.57 (1H, s, arH), 8.48 (1H, s, arH). ^{13}C NMR (DMSO- d_6 , δ ppm): 19.70 (CH_3), 20.25 (CH_2), 46.41 (CH_2), 47.03 (CH_2), 48.69 (CH_2), 49.78 (CH_2), 51.39 (CH_2), 53.78 (CH_2), 55.69 (CH_2), 57.23 (CH_2), 58.09 (CH_2), 59.11 (CH_2), arC: [119.85 (CH), 120.21 (CH), 121.58 (CH), 122.03 (CH), 125.79 (CH), 130.52 (C)], 161.20 (triazole C-3), 162.78 (triazole C-5). EI MS m/z (%): 403.89 ([M+1] $^+$, 100), 298.78 (85), 170.12 (51).

4-benzyl-5-((4-methylpiperazin-1-yl)methyl)-2-((4-phenylpiperazin-1-yl)methyl)-2H-1,2,4-triazole-3(4H)-thione (6b)

Yield: % 76, m.p: 183.185°C. FT IR (ν_{max} , cm^{-1}): 3073 (aromatic CH), 1589 (C=N). ^1H NMR (DMSO- d_6 , δ ppm): 2.60 (3H, d, J = 4.0 Hz, CH_3), 2.95 (2H, d, J = 4.0 Hz, CH_2), 2.99 (2H, s, CH_2), 3.14 (2H, s, CH_2), 3.15 (2H, s, CH_2), 3.42 (12H, s, 6 CH_2), 5.13 (2H, s, CH_2), 6.77 (1H, s, arH), 6.92 (3H, d, J = 8.0 Hz, arH), 7.21-7.26 (4H, m, arH), 7.54-7.59 (1H, s, arH), 8.45 (1H, s, arH). ^{13}C NMR (DMSO- d_6 , δ ppm): 17.22 (CH_3), 46.07 (CH_2), 47.53 (CH_2), 48.67 (CH_2), 49.09 (CH_2), 50.51 (CH_2), 51.79 (CH_2), 52.65 (CH_2), 53.64 (CH_2), 56.79 (CH_2), 57.98 (CH_2), 60.49 (CH_2), arC: [117.89 (CH), 118.69 (CH), 119.43 (CH), 120.31 (CH), 121.96 (CH), 122.49 (CH), 123.10 (CH), 125.80 (CH), 126.98 (CH), 129.03 (CH), 130.78 (C), 133.59 (C)], 165.90 (triazole C-3), 167.59 (triazole C-5). EI MS m/z (%): 478.69 ([M+1] $^+$, 100), 219.46 (87), 173.41 (45).

4-benzyl-2-((furan-2-ylmethylamino)methyl)-5-((4-methylpiperazin-1-yl)methyl)-2H-1,2,4-triazole-3(4H)-thione (6c)

Yield: % 78, m.p: 178-180°C. FT IR (ν_{max} , cm^{-1}): 3210 (OH), 3093 (aromatic CH), 1585 (C=N). ^1H NMR (DMSO- d_6 , δ ppm): 1.63 (3H, s, CH_3), 2.74 (2H, s, CH_2), 2.90 (2H, s, CH_2), 3.13 (2H, s, CH_2), 3.33 (2H, s, CH_2), 3.41 (4H, s, 2 CH_2), 3.62 (2H, s, CH_2), 4.17 (2H, s, CH_2), 7.26-7.33

(5H, m, arH), 7.96 (1H, s, CH), 13.82 (1H, s, NH). ^{13}C NMR (DMSO-*d*₆, δ ppm): 16.10 (CH₃), 45.21 (CH₂), 46.52 (CH₂), 47.41 (CH₂), 48.96 (CH₂), 50.23 (CH₂), 51.73 (CH₂), 53.59 (CH₂), 54.90 (CH₂), arC: [110.52 (CH), 112.36 (CH), 114.78 (CH), 115.37 (CH), 123.70 (CH), 139.07 (C), 142.43 (C)], 163.89 (triazole C-3), 164.70 (triazole C-5). EI MS *m/z* (%): 413.87 ([M+1]⁺, 100), 199.10 (66), 163.41 (49), 110.12 (31).

7-((4-benzyl-3-((4-methylpiperazin-1-yl)methyl)-5-thioxo-4,5-dihydro-1,2,4-triazol-1-yl)methyl)piperazin-1-yl)-1-ethyl-6-fluoro-4-oxo-1,4-dihydroquinoline-3-carboxylic acid (6d)

Yield: % 89, m.p: 242-244°C. FT IR (ν_{max} , cm⁻¹): 3410 (OH), 3095 (aromatic CH), 1699 (C=O), 1725 (C=O), 1582 (C=N). ^1H NMR (DMSO-*d*₆, δ ppm): 1.40 (3H, s, CH₃), 2.73 (3H, s, CH₃), 2.89 (4H, s, 2CH₂), 3.03 (4H, s, 2CH₂), 3.34 (8H, s, 4CH₂), 4.59 (4H, s, 2CH₂), 5.16 (4H, s, 2CH₂), 6.93 (1H, s, arH), 7.25 (1H, s, arH), 7.48 (1H, s, arH), 7.87-7.90 (2H, m, arH), 8.48 (1H, s, arH), 8.93 (1H, s, CH), 15.35 (1H, s, OH). ^{13}C NMR (DMSO-*d*₆, δ ppm): 11.20 (CH₃), 17.52 (CH₃), 45.23 (CH₂), 45.98 (CH₂), 46.19 (CH₂), 46.89 (CH₂), 50.51 (CH₂), 51.97 (CH₂), 52.10 (CH₂), 52.88 (CH₂), 53.41 (CH₂), 54.41 (CH₂), 55.79 (CH₂), 56.70 (CH₂), arC: [113.52 (CH), 114.79 (CH), 115.28 (CH), 117.34 (CH), 118.61 (CH), 119.39 (CH), 120.31 (CH), 128.41 (C), 129.80 (C), 130.76 (C), 131.31 (C), 132.70 (C), 133.74 (C)], 161.67 (triazole C-3), 163.79 (triazole C-5), 170.46 (C=O), 173.52 (C=O). EI MS *m/z* (%): 635.78 ([M+1]⁺, 100), 510.42 (88), 413.89 (71), 217.52 (43).

7-((4-benzyl-3-((4-methylpiperazin-1-yl)methyl)-5-thioxo-4,5-dihydro-1,2,4-triazol-1-yl)methyl)piperazin-1-yl)-1-cyclopropyl-6-fluoro-4-oxo-1,4-dihydroquinoline-3-carboxylic acid (6e)

Yield: % 91, m.p: 238-240°C. FT IR (ν_{max} , cm⁻¹): 3421 (OH), 3089 (aromatic CH), 1703 (C=O), 1718 (C=O, 1578 (C=N). ^1H NMR (DMSO-*d*₆, δ ppm): 1.16 (3H, s, CH₃), 1.30 (2H, s, CH₂), 1.32 (2H, s, CH₂), 3.05 (2H, s, CH₂), 3.37 (2H, s, CH₂), 3.80 (14H, s, 7CH₂), 5.16 (2H, s, CH₂), 6.94 (1H, s, arH), 7.23-7.27 (2H, s, arH), 7.49-7.59 (2H, s, arH), 7.87-7.90 (2H, m, arH), 8.46 (1H, s, CH), 8.65 (1H, s, CH), 15.20 (1H, s, OH). ^{13}C NMR (DMSO-*d*₆, δ ppm): 13.41 (CH₃),

46.10 (CH₂), 47.13 (CH₂), 48.48 (CH₂), 49.11 (CH₂), 50.03 (CH₂), 50.77 (CH₂), 51.13 (CH₂), 52.78 (CH₂), 53.90 (CH₂), 54.78 (CH₂), 55.13 (CH₂), 56.41 (CH₂), 58.03 (CH₂), arC: [112.70 (CH), 113.90 (CH), 115.03 (CH), 116.70 (CH), 119.63 (CH), 120.09 (CH), 121.10 (CH), 130.70 (C), 131.52 (C), 132.08 (C), 133.70 (C), 135.78 (C), 136.10 (C)], 159.20 (triazole C-3), 160.41 (triazole C-5), 172.52 (C=O), 174.96 (C=O). EI MS *m/z* (%): 647.89 ([M+1]⁺, 100), 488.10 (73), 310.41 (51), 170.43 (31).

2-(4-benzyl-3-((4-methylpiperazin-1-yl)methyl)-5-thioxo-4,5-dihydro-1,2,4-triazol-1-yl)-1-(4-chlorophenyl)ethanone (7)

The solution of products 5 (10 mmol) and sodium ethoxid (1 mmol) in 10 mL of ethanol was refluxed for 6 h. After that 2-bromo-1-(4-chlorophenyl)ethanone (10 mmol) was added into it, and the solution was refluxed for a 16 h. After evaporation the solvent under reduced pressure, a crude acquired. The crude substance was collected by filtration and recrystallized from acetone:water (1:3) to the acquired desired molecules.

Yield: % 90, m.p: 203-205 °C. FT IR (ν_{max} , cm⁻¹): 3097 (aromatic CH), 1725 (C=O), 1598 (C=N). ¹H NMR (DMSO-*d*₆, δ ppm): 2.27 (3H, d, *J*= 4.0 Hz, CH₃), 2.40 (2H, s, CH₂), 2.55 (2H, d, *J*= 4.0 Hz, CH₂), 3.39 (2H, s, CH₂), 4.39 (2H, s, CH₂), 4.57 (2H, s, CH₂), 5.10 (2H, s, CH₂), 5.48 (2H, s, CH₂), 7.19 (1H, s, arH), 7.20 (1H, s, arH), 7.26 (1H, s, arH), 7.26 (1H, s, arH), 7.35 (1H, s, arH), 7.63 (1H, s, arH). ¹³C NMR (DMSO-*d*₆, δ ppm): 20.14 (CH₃), 45.98 (CH₂), 46.01 (CH₂), 47.13 (CH₂), 48.36 (CH₂), 49.48 (CH₂), 50.79 (CH₂), 51.29 (CH₂), arC: [113.52 (CH), 114.42 (CH), 119.43 (CH), 120.12 (CH), 121.49 (CH), 123.20 (CH), 124.80 (CH), 127.94 (CH), 129.43 (CH), 134.12 (C), 136.41 (C), 137.49 (C)], 151.14 (triazole C-3), 156.79 (triazole C-5), 171.10 (C=O). EI MS *m/z* (%): 456.12 ([M+1]⁺, 100), 288.12 (78), 197.12 (51).

4-benzyl-2-(2-(4-chlorophenyl)-2-hydroxyethyl)-5-((4-methylpiperazin-1-yl)methyl)-2H-1,2,4-triazole-3(4H)-thione (8)

A solution of the corresponding compound 7 (10 mmol) in absolute ethanol (50 mL) was refluxed in the presence of NaBH₄ (30 mmol) for 18 h. After evaporating the solvent

under reduced pressure, an oily mass appeared. This was recrystallized from acetone: water (1:3) to afford desired product.

Yield: % 71, m.p: 128-130 $^{\circ}\text{C}$. FT IR (ν_{max} , cm^{-1}): 3319 (OH), 3078 (aromatic CH), 1585 (C=N). ^1H NMR (DMSO- d_6 , δ ppm): 2.30 (3H, s, CH_3), 2.44 (2H, s, CH_2), 2.48 (4H, s, 2 CH_2), 2.68 (2H, s, CH_2), 4.09 (2H, s, CH_2), 4.63 (2H, s, CH_2), 4.84 (2H, s, CH_2), 4.84 (2H, s, CH_2), 4.97 (1H, s, CH), 5.26 (1H, s, OH), 7.02 (1H, s, arH), 7.16 (1H, s, arH), 7.18 (1H, s, arH), 7.25 (2H, s, arH), 7.28 (2H, s, arH), 7.36 (2H, s, arH). ^{13}C NMR (DMSO- d_6 , δ ppm): 20.90 (CH_3), 39.12 (CH_2), 46.56 (CH_2), 47.41 (CH_2), 49.03 (CH_2), 49.95 (CH_2), 50.07 (CH_2), 51.59 (CH_2), 126.12 (CH), arC: [130.12 (CH), 131.19 (CH), 132.85 (CH), 133.76 (CH), 134.09 (CH), 135.90 (CH), 136.98 (CH), 137.12 (C), 138.90 (C), 140.52 (C)], 153.70 (triazole C-3), 155.97 (triazole C-5). EI MS m/z (%): 458.90 ([M+1] $^+$, 100), 311.89 (73), 298.10 (55), 170.12 (41).

2-(2-(4-chlorobenzyl)oxy)-2-(4-chlorophenyl)ethyl)-4-benzyl-5-((4-methylpiperazin-1-yl)methyl)-2H-1,2,4-triazole-3(4H)-thione (9)

The addition of NaH (1 mmol) to a solution of compound 8 (1 mmol) in tetrahydrofuran was followed by 6 h of reflux heating. To the mixture was then added the appropriate benzyl chloride and the mixture was refluxed for an additional 8–12 h. Following concentration under reduced pressure, the resulting oily mass was treated with a solution of K_2CO_3 (1 mmol) and the combination was extracted with ethyl acetate (3X15 mL). Na_2SO_4 was used to dry the organic layer, which was then concentrated under reduced pressure. Acetone was used to crystallize the residue.

Yield: % 58, m.p: 69-71 $^{\circ}\text{C}$. FT IR (ν_{max} , cm^{-1}): 3055 (aromatic CH), 3092 (aromatic CH), 1579 (C=N). ^1H NMR (DMSO- d_6 , δ ppm): 2.27 (3H, s, CH_3), 2.36 (2H, s, CH_2), 2.39 (4H, s, 2 CH_2), 2.57 (2H, s, CH_2), 3.83 (2H, s, CH_2), 4.45 (2H, s, CH_2), 4.58 (2H, s, CH_2), 4.65 (2H, s, CH_2), 4.85 (1H, s, CH), 5.08 (1H, s, OH), 7.14-7.19 (7H, m, arH), 7.25-7.26 (6H, m, arH). ^{13}C NMR (DMSO- d_6 , δ ppm): 23.07 (CH_3), 40.63 (CH_2), 47.90 (CH_2), 48.66 (CH_2), 49.12 (CH_2), 50.88 (CH_2), 51.23 (CH_2), 52.44 (CH_2), 56.37 (CH_2), 119.10 (CH), arC: [121.53 (CH), 123.20 (CH), 124.33 (CH), 126.50 (CH), 127.81 (CH), 128.64 (CH), 129.40 (CH), 134.39 (CH), 135.70

(CH), 136.86 (CH), 139.40 (CH), 141.33 (CH), 142.50 (CH), 143.23 (C), 144.03 (C), 145.30 (C), 146.23 (C), 147.34 (C), 148.78 (C)], 156.89 (triazole C-3), 157.13 (triazole C-5). EI MS *m/z* (%): 582.29 ([M+1]⁺, 100), 389.25 (73), 219.46 (57), 188.90 (40).

Declarations

Conflict of interest On behalf of all authors, the corresponding author states that there is no conflict of interest.

References

- [1] E. Weiderpass, D. Hashim, F. Labrèche, Malignant tumors of the female reproductive system, in: *Occupational Cancers*, Springer International Publishing, Cham, 2020, pp. 439–453, doi: 10.1007/978-3-030-30766-0_25
- [2] M. Arbyn, E. Weiderpass, L. Bruni, S. de Sanjose, M. Saraiya, J. Ferlay, F. Bray, Estimates of incidence and mortality of cervical cancer in 2018: a worldwide analysis, *Lancet Glob. Health* 8 (2020) e191–e203, doi: 10.1016/S2214-109X(19)30482-6.
- [3] F. Ordikhani, M.E. Arslan, R. Marcelo, I. Sahin, P. Grigsby, J.K. Schwarz, A.K. Azab, Drug delivery approaches for the treatment of cervical cancer, *Pharmaceutics* 8 (2016) 23, doi: 10.3390/pharmaceutics8030023.
- [4] A.C. Chrysostomou, D.C. Stylianou, A. Constantinidou, L.G. Kostrikis, Cervical cancer screening programs in Europe: the transition towards HPV vaccination and population-based HPV testing, *Viruses* 10 (2018) 729, doi: 10.3390/v10120729.
- [5] M. Gatumo, S. Gacheri, A.R. Sayed, A. Scheibe, Women's knowledge and attitudes related to cervical cancer and cervical cancer screening in Isiolo and Tharaka Nithi counties, Kenya: a cross-sectional study, *BMC Cancer* 18 (2018) 745, doi: 10.1186/s12885-018-4642-9.
- [6] R.J. DeBerardinis, J.J. Lum, G. Hatzivassiliou, C.B. Thompson, The biology of cancer: metabolic reprogramming fuels cell growth and proliferation, *Cell Metab.* 7 (2008) 11–20, doi: 10.1016/j.cmet.2007.10.002.
- [7] N. Pediconi, F. Ghirga, C. Del Plato, G. Peruzzi, C. M. Athanassopoulos, M. Mori, M. E. Crestoni, D. Corinti, F. Ugozzoli, C. Massera, et al. “Design and Synthesis of Piperazine-Based Compounds Conjugated to Humanized Ferritin as Delivery System of siRNA in Cancer Cells,” *Bioconjugate Chemistry* 32, no. 6(2021): 1105–16.
- [8] M. X. Wei, J. Y. Yu, X. X. Liu, X. Q. Li, M. W. Zhang, P. W. Yang, and J. H. Yang, “Synthesis of Artemisinin-Piperazine-Furan Ether Hybrids and Evaluation of in Vitro Cytotoxic Activity,” *European Journal of Medicinal Chemistry* 215 (2021): 113295.
- [9] M. Patil, A. Noonikara-Poyil, S. D. Joshi, S. A. Patil, S. A. Patil, A. M. Lewis, and A. Bugarin, “Synthesis, Molecular Docking Studies, and in Vitro Antimicrobial Evaluation of Piperazine and Triazolo-PyrazineDerivatives,” *Molecular Diversity* (2021): 1–15. doi:10.1007/s11030-021-10190-x

[10] R. R. Kumar, B. Sahu, S. Pathania, P. K. Singh, M. J. Akhtar, and B. Kumar, “Piperazine, a Key Substructure for Antidepressants: Its Role in Developments and Structure-Activity Relationships,” *ChemMedChem* 16, no.12 (2021): 1878–901.

[11] R. Abu Khalaf, H. Abu Jarad, T. Al-Qirim, and D. Sabbah, “Synthesis, Biological Evaluation, and QPLD Studies of Piperazine Derivatives as Potential DPP-IV Inhibitors,” *Medicinal Chemistry* 17, no. 9 (2021): 937–44.

[12] M. F. Ahmed, E. Y. Santali, and R. El-Haggar, “Novel Piperazine-Chalcone Hybrids and Related Pyrazoline Analogues Targeting VEGFR-2 Kinase; Design, Synthesis, Molecular Docking Studies, and Anticancer Evaluation,” *Journal of Enzyme Inhibition and Medicinal Chemistry* 36, no. 1 (2021): 307–18.

[13] M. Al-Ghorbani, G. S. Pavankumar, P. Naveen, P. Thirusangu, B. T. Prabhakar, and S. A. Khanum, “Synthesis and an Angiolytic Role of Novel Piperazine-Benzothiazole Analogues on Neovascularization, a Chief Tumoral Parameter in Neoplastic Development,” *Bioorganic Chemistry* 65 (2016): 110–7.

[14] Y. A. Al-Soud, A. H. Al-Ahmad, L. Abu-Qatouseh, A. Shtaiwi, K. A. S. Alhelal, H. H. Al-Suod, S. O. Alsawakhneh, and R. A. Al-Qawasmeh, “Nitroimidazoles Part 9. Synthesis, Molecular Docking, and Anticancer Evaluations of Piperazine-Tagged Imidazole Derivatives,” *Zeitschrift für Naturforschung B* 76, no.5 (2021): 293–302.

[15] M. Al-Ghorbani, N. D. Rekha, V. Lakshmi Ranganatha, T. Prashanth, T. Veerabasappagowda, and S. A. Khanum, “Synthesis and Biological Efficacy of Novel Piperazine Analogues Bearing Quinoline and Pyridine Moieties,” *Russian Journal of Bioorganic Chemistry* 41, no. 5 (2015): 554–61.

[16] W. Li, S.-Y. Chen, W.-N. Hu, M. Zhu, J.-M. Liu, Y.-H. Fu, Z.-C. Wang, and G.-P. OuYang, “Design, Synthesis, and Biological Evaluation of Quinazoline Derivatives Containing Piperazine Moieties as Antitumor Agents,” *Journal of Chemical Research* 44, no. 9-10 (2020): 536–42.

[17] K. Ostrowska, “Coumarin-Piperazine Derivatives as Biologically Active Compounds,” *Saudi Pharmaceutical Journal* 28, no. 2 (2020): 220–32.

[18] Kerns, R. J.; Rybak, M. J.; Kaatz, G. W.; Vaka, F.; Cha, R.; Grucz, R. G.; Diwadkar, V. U. Structural Features of Piperazinyl-Linked Ciprofloxacin Dimers Required for Activity against Drug-Resistant Strains of *Staphylococcus aureus*. *Bioorganic Med. Chem. Lett.* 2003, 13, 2109–2112. DOI: 10.1016/S0960-894X(03)00376-7.

[19] Upadhyaya, R. S.; Sinha, N.; Jain, S.; Kishore, N.; Chandra, R.; Arora, S. K. Optically Active Antifungal Azoles: Synthesis and Antifungal Activity of (2R,3S)-2-(2,4-Difluorophenyl)-3-(5-[2-[4-Aryl-Piperazin-1-yl]-Ethyl]-Tetrazol-2-yl/1-yl)-1-[1,2,4]-Triazol-1-yl-Butan-2-ol. *Bioorg. Med. Chem.* 2004, 12, 2225–2238. DOI: 10.1016/j.bmc.2004.02.014.

[20] Suryavanshi, H. R.; Rathore, M. M. Synthesis and Biological Activities of Piperazine Derivatives as Antimicrobial and Antifungal Agents. *Org. Commun.* 2017, 10, 228–238. DOI: 10.25135/acg.oc.23.17.05.026.

[21] Chaudhary, P.; Kumar, R.; Verma, A. K.; Singh, D.; Yadav, V.; Chhillar, A. K.; Sharma, G. L.; Chandra, R. Synthesis and Antimicrobial Activity of N-Alkyl and N-Aryl Piperazine Derivatives. *Bioorg. Med. Chem.* 2006, 14, 1819–1826. DOI: 10.1016/j.bmc.2005.10.032.

[22] Martin, R. J. Modes of Action of Anthelmintic Drugs. *Veterinary J.* 1997, 154, 11–34. DOI: 10.1016/S1090-0233(05)80005-X.

[23] Kharb, R.; Bansal, K.; Sharma, A. K. A Valuable Insight into Recent Advances on Antimicrobial Activity of Piperazine Derivatives. *Der Pharma Chem.* 2012, 4, 2470–2488.

[24] R.-H. Zhang, H.-Y. Guo, H. Deng, J. Li, Z.-S. Quan, J. Enzyme Inhib. *Med. Chem.* 2021, 36(1), 1165.

[25] M. Al-Ghorbani, A. Bushra Begum, Z. Zabiulla, S. V. Mamatha, S. A. Khanum, *Res. J. Pharm. Technol.* 2015, 8(5), 611.

[26] R. V. Patel, S. Won Park, *Mini Rev. Med. Chem.* 2013, 13(11), 1579.

[27] M. Shaquiquzzaman, G. Verma, A. Marella, M. Akhter, W. Akhtar, M. F. Khan, S. Tasneem, M. M. Alam, *Eur. J. Med. Chem.* 2015, 102, 487.

[28] I. A. Moussa, S. D. Banister, C. Beinat, N. Giboureau, A. J. Reynolds, M. Kassiou, *J. Med. Chem.* 2010, 53(16), 6228.

[29] Y. He, F. Xie, J. Ye, W. Deuther-Conrad, B. Cui, L. Wang, J. Lu, J. Steinbach, P. Brust, Y. Huang, J. Lu, H. Jia, *J. Med. Chem.* 2017, 60(10), 4161.

[30] N. Sergeant, V. Vingtdeux, S. Eddarkaoui, M. Gay, C. Evrard, N. Le Fur, C. Laurent, R. Caillierez, H. Obriot, P. E. Larchanché, A. Farce, M. Coevoet, P. Carato, M. Kouach, A. Descat, P. Dallemande, V. Buée-Scherrer, D. Blum, M. Hamdane, L. Buée, P. Melnyk, *Neurobiol. Dis.* 2019, 129, 217.

[31] Q. Ji, Q. Deng, B. Li, B. Li, Y. Shen, *Eur. J. Med. Chem.* 2019, 180, 204.

[32] F.R. Benson, W.L. Savell, The chemistry of the vicinal triazoles, *Chem. Rev.* 46 (1) (1950) 1–68 .

[33] A. Czyrski, et al., The overview on the pharmacokinetic and pharmacodynamic interactions of triazoles, *Pharmaceutics* 13 (11) (2021) 1961 .

[34] J.K. Sahu, S. Ganguly, A. Kaushik, Triazoles: a valuable insight into recent developments and biological activities, *Chin. J. Nat. Med.* 11 (5) (2013) 456–465 .

[35] K. Shalini, et al., Advances in synthetic approach to and antifungal activity of triazoles, *Beilstein J. Org. Chem.* 7 (1) (2011) 668–677 .

[36] P.P. Gadhav, et al., Current biological and synthetic profile of triazoles: a review, *Annals Biol. Res* (1) (2010) 82–89 .

[37] I. Pibiri, S. Buscemi, A recent portrait of bioactive triazoles, *Curr. Bioact. Compd.* 6 (4) (2010) 208–242 .

[38] S. V. Tiwari, J. A. Seijas, M. P. Vazquez-Tato, A. P. Sarkate, K. S. Karnik, A. P. G. Nikalje, *Molecules* 2018, 23(2), 1.

[39] S. Ke, L. Shi, Z. Yang, *Bioorg. Med. Chem. Lett.* 2015, 25(20), 4628.

[40] Z. Xu, S. J. Zhao, Z. S. Lv, F. Gao, Y. Wang, F. Zhang, L. Bai, J. L. Deng, *Eur. J. Med. Chem.* 2019, 162, 396.

[41] A. S. Hassan, G. O. Moustafa, H. M. Awad, E. S. Nossier, M. F. Mady, *ACS Omega* 2021, 6(18), 12361.

[42] P. A. Willanova, *NCCLS Document M7-A3* 1993, 13, 25.

[43] N. Ke, X. Wang, X. Xu, Y. A. Abassi, *Mol. Biol.* 2011, 740, 33.

[44] G. Abay, M. Altun, S. Koldas, A. R. Tufekci, I. Demirtas, *Comb. Chem. High. Througt. Screen.* 2015, 18, 453.

[45] Zhao, Y. J.; Wei, W.; Su, Z. G.; Ma, G. H. Poly(ethylene glycol) prodrug for anthracyclines via N-Mannich base linker: design, synthesis and biological evaluation. *Int. J. Pharm.* 2009, 379, 90–99.

[46] Roman, O. G. Mannich bases in medicinal chemistry and drug design. *Eur. J. Med. Chem.* 2015, 89, 743–816.

[47] Ganiyat, K.; Willie, I. E.; Oluwakemi, O. Synthesis of Mannich bases: 2-(3-Phenylaminopropionyloxy)-benzoic acid and 3-phenylamino-1-(2, 4, 6-trimethoxy-phenyl)propan-1- one, their toxicity, ionization constant, antimicrobial and antioxidant activities. *Food Chem.* 2014, 165, 515–521.

[48] Fekner, T.; Baldwin, J. E.; Adlington, R. M.; Fardeau, S.; Jones, T. W.; Prout, C. K.; Schofield, C. J. Synthesis of (6S)-cephalosporins from 6-aminopenicillanic acid. *Tetrahedron* 2000, 56, 6053–6074.

[49] Dassonville-Klimpt, A.; Audic, N.; Sasaki, A.; Pillon, M.; Baudrin, E.; Mullié, C.; Sonnet, P. Synthesis and antibacterial activity of catecholate-ciprofloxacin conjugates. *Bioorg. Med. Chem.* 2014, 22, 4049–4060.

Supplementary Files

This is a list of supplementary files associated with this preprint. Click to download.

- [Suplementarydata.docx](#)